Simulation-Based Variance Components Analysis for Characterization of Interaction Effects of Random Factors on Trichloroethylene Vapor Transport in Unsaturated Porous Media

ARTICLE *in* INDUSTRIAL & ENGINEERING CHEMISTRY RESEARCH · JUNE 2013

Impact Factor: 2.59 · DOI: 10.1021/ie4012003

4 AUTHORS, INCLUDING:

Shuo Wang
University of Regina
29 PUBLICATIONS **218** CITATIONS

SEE PROFILE

I&EC research
Industrial & Engineering Chemistry Research

Article

pubs.acs.org/IECR

Simulation-Based Variance Components Analysis for Characterization of Interaction Effects of Random Factors on Trichloroethylene Vapor Transport in Unsaturated Porous Media

S. Wang,[†] Guo H. Huang,*[,†] J. Wei,[†] and L. He[‡]

[†]Faculty of Engineering and Applied Science, University of Regina, Regina, Saskatchewan, Canada S4S 0A2

[‡]MOE Key Laboratory of Regional Energy and Environmental Systems Optimization, Resources and Environmental Research Academy, North China Electric Power University, Beijing 102206, China

Supporting Information

ABSTRACT: This paper presents a simulation-based random effects model for analyzing the interaction effects of random factors on the gaseous transport of volatile organic compounds (VOCs) in the unsaturated zone. The model has the advantages of addressing parameter uncertainty characterized by inherent randomness in simulating the gaseous transport of VOCs in the unsaturated porous media, as well as of investigating their potential interactions and the nonlinear effects on the VOC vapor concentrations through a variance components analysis. The proposed model is applied to a numerical experiment on the transport behavior of trichloroethylene (TCE) vapors in the unsaturated porous media. The results reveal that variations of random factors can cause a significant difference in the gaseous TCE concentrations, and the temporal and spatial variability in the TCE vapor concentrations can result in different effects of factors on the model response.

1. INTRODUCTION

Soil and groundwater contamination by volatile organic compounds (VOCs) has become an issue of great concern in many industrialized countries. The most common cause of contamination is accidental spills or leakages of VOCs as nonaqueous phase liquids (NAPLs).[1] During the migration of NAPLs through the unsaturated zone, a certain amount of these liquids will be retained as residual saturation in the soil by capillary forces.[2] Since the residual NAPL volatiles into soil gas and dissolves into groundwater as the result of kinetic mass transfer processes, it becomes a long-lasting contaminant source, causing potential ecological and human health risks.[3]

In the unsaturated zone, the gas phase transport of VOCs has been identified as an important process contributing to groundwater contamination, spreading of contaminants, and contaminant release to the atmosphere.[4] The movement of the vapor plume is influenced by various transport mechanisms, including advection, diffusion, and dispersion in the gas phase.[5] Numerical modeling is recognized as a powerful means to characterize the gaseous transport behavior of VOCs in the subsurface. In the past, a number of mathematical models were developed to investigate the gas-phase transport of VOCs in the unsaturated zone.[6−15]

Although many previous studies took advantage of the numerical models as an effective means to gain an in-depth insight into the complex mechanisms of the transport process of VOCs in the gas phase, they hardly took into account the interaction effects of input parameters on the model outputs. In fact, certain parameters may interact in significant ways and have a remarkable influence on the gaseous transport behavior of VOCs. It is thus necessary to analyze their potential interactions and the resulting effects on the model response.

Over the past decade, factorial experiments have been widely used to study the combined effects of two or more factors on the response variable.[16−24] Previous studies mainly focused on the investigation of effects of fixed factors with their levels being specified deliberately, implying that statistical inferences made about these factors were confined to the specific levels studied.

However, random factors are frequently encountered in practice; they have a large number of possible levels rather than several specific levels. Therefore, the objective of this study is to propose a simulation-based random effects model for analyzing the interaction effects of random factors on the gaseous transport of VOCs within the unsaturated zone.

To illustrate the proposed model, a numerical experiment will be used to characterize the transport behavior of TCE vapors originating from a residual TCE source zone in the unsaturated porous media. The results obtained from the random effects model will also be compared to those from the fixed effects model, which is meaningful for providing an in-depth analysis of the difference between the fixed and random effects models.

2. METHODOLOGY

2.1. Simulation Model. A mathematical and numerical model developed by Guarnaccia et al.[25] is recognized as an effective tool in simulating the transport and fate of NAPLs in near-surface granular soils. The simulation model is capable not only of accommodating three mobile phases: water, NAPL, and gas, but also of addressing three fundamental, interrelated, and physical processes that occur in the subsurface: multiphase flow,

Received: April 15, 2013
Revised: May 23, 2013
Accepted: June 4, 2013
Published: June 4, 2013

dx.doi.org/10.1021/ie4012003 | *Ind. Eng. Chem. Res.* 2013, 52, 8602−8611

interphase mass transfer, and constituent mass transport. Thus, it was used in this study for characterizing the gaseous TCE transport behavior in the subsurface.

The basic mass conservation equation for components in the subsurface can be written as follows:[26]

$$\frac{\partial}{\partial t}(\varepsilon S_\alpha \rho_\alpha^\iota) + \nabla\cdot[\varepsilon S_\alpha \rho_\alpha^\iota \nu_\alpha] - \nabla\cdot\left[\varepsilon S_\alpha \rho_\alpha D_\alpha \cdot \nabla\left(\frac{\rho_\alpha^\iota}{\rho_\alpha}\right)\right] + \varepsilon S_\alpha \kappa_\alpha^\iota \rho_\alpha^\iota = \rho_\alpha^\iota Q_\alpha + \hat{\rho}_\alpha^\iota \quad (1)$$

where α is the phase index (W = water, N = NAPL, G = gas, S = solid); ι is the component index (w = water, n = NAPL, g = gas); ε is the porosity of porous medium; S_α is the saturation of phase α; ρ_α^ι is the mass concentration of component ι in phase α [M L^{-3}]; ν_α is the mass average velocity of phase α, a vector [L T^{-1}]; D_α is the dispersion coefficient for the α-phase, a symmetric second-order tensor [L^2 T^{-1}]; Q_α is the point source (+) or sink (−) of the α-phase mass [T^{-1}]; k_α^ι is the decay coefficient for component ι in phase α [T^{-1}]; $\hat{\rho}_\alpha^\iota$ is the source or sink of mass for component ι in phase α [M L^{-3} T^{-1}] due to interphase mass exchange (i.e., dissolution, volatilization, and adsorption). The dispersion tensor can be represented as[27]

$$D_{\iota\alpha ij} = \frac{D_{m,\iota\alpha}}{\tau}\delta_{ij} + \frac{a_{T\alpha}}{\varepsilon S_\alpha}|\nu_\alpha|\delta_{ij} + \frac{(a_{L\alpha} - a_{T\alpha})}{\varepsilon S_\alpha}\frac{\nu_{\alpha i}\nu_{\alpha j}}{|\nu_\alpha|} \quad (2)$$

where τ is the tortuosity effect (defined with a value greater than 1); $D_{m,\iota\alpha}$ is the molecular diffusion coefficient of component ι in phase α [L^2 T^{-1}]; δ_{ij} is the Kronecker delta function; $a_{L\alpha}$ is the longitudinal dispersivity [L]; $a_{T\alpha}$ is the transverse dispersivity [L]; $v_{\alpha i}$ and $v_{\alpha j}$ are the components of Darcy velocity in directions i and j, respectively [L T^{-1}]; $|v_\alpha|$ is the magnitude of flux for phase α [LT^{-1}]. The phase flux can be described in the multiphase form of Darcy's law:[28]

$$\nu_\alpha = -\frac{\mathrm{k}k_{r\alpha}}{\mu_\alpha}(\nabla P_\alpha - \rho_\alpha g \nabla z), \quad \alpha = \mathrm{W, N, G} \quad (3)$$

where k is the intrinsic permeability tensor [L^2]; $k_{r\alpha}$ is the relative permeability of phase α; μ_α is the viscosity of phase α [M L^{-2} T^{-1}]; P_α is the α-phase pressure [M L^{-1} T^{-2}]; ρ_α is the density of phase α [M L^{-3}]; g is the acceleration due to gravity [L T^{-2}]; z is the vertical distance, which is defined as positive downward [L]. To ensure mass conservation, the preceding equations are subject to the constraints:[25]

$$S_\mathrm{W} + S_\mathrm{N} + S_\mathrm{G} = 1 \quad (4)$$

$$\rho_\alpha = \sum_{\iota=\mathrm{w,n,g}} \rho_\alpha^\iota, \quad \alpha = \mathrm{W, N, G} \quad (5)$$

$$\hat{\rho}_\alpha = \sum_{\iota=\mathrm{w,n,g}} \hat{\rho}_\alpha^\iota, \quad \alpha = \mathrm{W, N, G} \quad (6)$$

$$\sum_{\alpha=\mathrm{W,N,G}} \hat{\rho}_\alpha = 0 \quad (7)$$

$$\sum_{\iota=\mathrm{w,n,g}} \kappa_\alpha^\iota \rho_\alpha^\iota = 0, \quad \alpha = \mathrm{W, N, G} \quad (8)$$

where ρ_α and $\hat{\rho}_\alpha$ are the α-phase mass density [M L^{-3}] and the total mass change in phase α, respectively. With the aid of the numerical model, the physical problem can be cast into a mathematical representation consisting of five mass balance equations. The first three fluid-phase (i.e., water-, NAPL-, and gas-phases) balance equations can be described by[25]

$$\frac{\partial}{\partial t}(\varepsilon S_\mathrm{W}\rho_\mathrm{W}) + \nabla\cdot[\varepsilon S_\mathrm{W}\rho_\mathrm{W}\nu_\mathrm{W}] = \rho_\mathrm{W}Q_\mathrm{W} + E_\mathrm{W}^n - E_\mathrm{G}^{\mathrm{n/W}} - E_\mathrm{S}^{\mathrm{n/W}} \quad (9)$$

$$\frac{\partial}{\partial t}(\varepsilon S_\mathrm{N}\rho_\mathrm{N}) + \nabla\cdot[\varepsilon S_\mathrm{N}\rho_\mathrm{N}\nu_\mathrm{N}] = \rho_\mathrm{N}Q_\mathrm{N} - E_\mathrm{W}^\mathrm{n} - E_\mathrm{G}^\mathrm{n} \quad (10)$$

$$\frac{\partial}{\partial t}(\varepsilon S_\mathrm{G}\rho_\mathrm{G}) + \nabla\cdot[\varepsilon S_\mathrm{G}\rho_\mathrm{G}\nu_\mathrm{G}] = \rho_\mathrm{G}Q_\mathrm{G} + E_\mathrm{G}^\mathrm{n} + E_\mathrm{G}^{\mathrm{n/W}} \quad (11)$$

where E_W^n represents the dissolution mass transfer of the NAPL components from the NAPL phase to the water phase; $E_\mathrm{G}^{\mathrm{n/W}}$ represents the volatilization mass transfer of the NAPL components from the water phase to the gas phase; E_G^n represents the volatilization mass transfer of the NAPL components from the NAPL phase to the gas phase; $E_\mathrm{S}^{\mathrm{n/W}}$ represents the adsorption mass transfer of the NAPL components from the water phase to the soil. The flow properties of water, NAPL, and gas phases can be defined through the three fluid-phase balance equations. The other two NAPL component balance equations characterize the transport of the NAPL components within and between different phases. The volatilization mass exchange term E_G^n can be given by[25]

$$E_\mathrm{G}^\mathrm{n} = C_\mathrm{G}^\mathrm{n}(\bar{\rho}_\mathrm{G}^\mathrm{n} - \rho_\mathrm{G}^\mathrm{n}) \quad (12)$$

where C_G^n is the rate coefficient, which regulates the rate at which equilibrium is reached [T^{-1}]; $\bar{\rho}_\mathrm{G}^\mathrm{n}$ is the constant equilibrium vapor concentration of the NAPL component in the gas phase [M T^{-3}]. The rate coefficient C_G^n is assumed to have the following form:[25]

$$C_\mathrm{G}^\mathrm{n} = \beta_\mathrm{GN}(\varepsilon S_\mathrm{N})^\beta \quad (13)$$

where $\beta \approx 0.5$ is the dimensionless fitting parameter; β_GN is fit to available experimental- or field-scale data [T^{-1}]. Different from the mass exchange term E_G^n, $E_\mathrm{G}^{\mathrm{n/W}}$ governs the volatilization mass transfer of a dissolved NAPL component in the water phase to the gas phase:[25]

$$E_\mathrm{G}^{\mathrm{n/W}} = C_\mathrm{G}^{\mathrm{n/W}}(H\rho_\mathrm{W}^\mathrm{n} - \rho_\mathrm{G}^\mathrm{n}) \quad (14)$$

where H is the dimensionless Henry's law coefficient and can be defined as follows:

$$H = \frac{\rho_\mathrm{G}^\mathrm{n}}{\rho_\mathrm{W}^\mathrm{n}} \quad (15)$$

and $C_\mathrm{G}^{\mathrm{n/W}}$ is the rate coefficient, which is defined by

$$C_\mathrm{G}^{\mathrm{n/W}} = \beta_\mathrm{GW}(\varepsilon S_\mathrm{W})^\beta \quad (16)$$

where $\beta \approx 0.5$ is the dimensionless fitting parameter; β_GN is fit to available data [T^{-1}].

The numerical model features an iterative sequential solution strategy for solving the governing equations and a Hermite collocation finite element method for discretizing the domain into a finite number of bricklike elements with nodes located at element boundary intersections. Such a model can provide an accurate solution of the coupled nonlinear partial differential equations that are generated by combining the fundamental mass balance equations with the constitutive and thermodynamic relationships.[25]

dx.doi.org/10.1021/ie4012003 | Ind. Eng. Chem. Res. 2013, 52, 8602−8611

2.2. Random Effects Model. Characterization of contaminant fate and transport in the subsurface requires extensive data and information that are associated with a variety of uncertainties. These uncertainties stem from many factors related to hydrogeological and physicochemical conditions.[29] These factors have different impacts on the model outputs and their variations can lead to a significant difference in predicted results. Besides, these factors are actually correlated with each other. Valuable information may be hidden beneath the potential interactions between factors and their resulting effects. It is thus imperative to investigate the interaction effects of factors and explore their hidden information.

The random effects model is proposed to analyze the influences of random factors on the model response and can be written as follows:[30]

$$y_{ij} = \mu + \tau_i + \varepsilon_{ij} \begin{cases} i = 1, 2, ..., m \\ j = 1, 2, ..., n \end{cases} \quad (17)$$

where μ is the overall mean; τ_i is the ith treatment effect; ε_{ij} is the random error. τ_i and ε_{ij} are the normally and independently distributed random variables with means zero and variances σ_τ^2 and σ^2, respectively. Variances σ_τ^2 and σ^2 are called variance components in the random effects model; the variance of any observation is

$$\sigma_y^2 = \sigma_\tau^2 + \sigma^2 \quad (18)$$

The total variability in the observations can be divided into a component that measures the differences between treatment means and a component that measures the differences of observations within a treatment from the treatment average. Thus, the overall variability in the data that can be measured by the total sum of squares is represented as

$$SS_{total} = SS_{between} + SS_{within} \quad (19)$$

where $SS_{between}$ is the sum of squares due to treatments; SS_{within} is the sum of squares due to error. To form the test statistics, the corresponding expected mean squares must be examined by[30]

$$E(MS_{between}) = \sigma^2 + n\sigma_\tau^2 \quad (20)$$

and

$$E(MS_{within}) = \sigma^2 \quad (21)$$

Estimating the variance components plays a crucial role in the random effects model. The analysis of variance method was used in this study to calculate the variance components, and their estimates were obtained by[30]

$$\hat{\sigma}_\tau^2 = \frac{MS_{between} - MS_{within}}{n} \quad (22)$$

and

$$\hat{\sigma}^2 = MS_{within} \quad (23)$$

where $\hat{\sigma}_\tau^2$ and $\hat{\sigma}^2$ represent the sources of variability between treatments and within treatments (error), respectively.

Figure 1 shows the flowchart of the procedures for solving the random effects model. It consists of 11 steps. First, a numerical experiment is characterized, including the model domain dimensions as well as initial and boundary conditions. Then random factors are identified. To ease the computational burden for performing the factorial experiment, random factors can be discretized into three interval ranges of low, medium, and high levels. Then three values can be randomly generated for each factor within these ranges to better represent a probability distribution. After that, the numerical model is run for each treatment combination in the factorial design. Thus, the simulation results can be obtained under different scenarios. Since the outputs of the simulation model can be used as inputs for the random effects model, statistical inferences can be made about the entire population of factor levels. Then the analysis of variance table is obtained, and the variance components are estimated through the analysis of variance method. Finally, the main and interaction effects of random factors are investigated thoroughly. Consequently, the random effects model is effective in dealing with random factors in a numerical experiment and revealing their effects on the model response in a systematical manner.

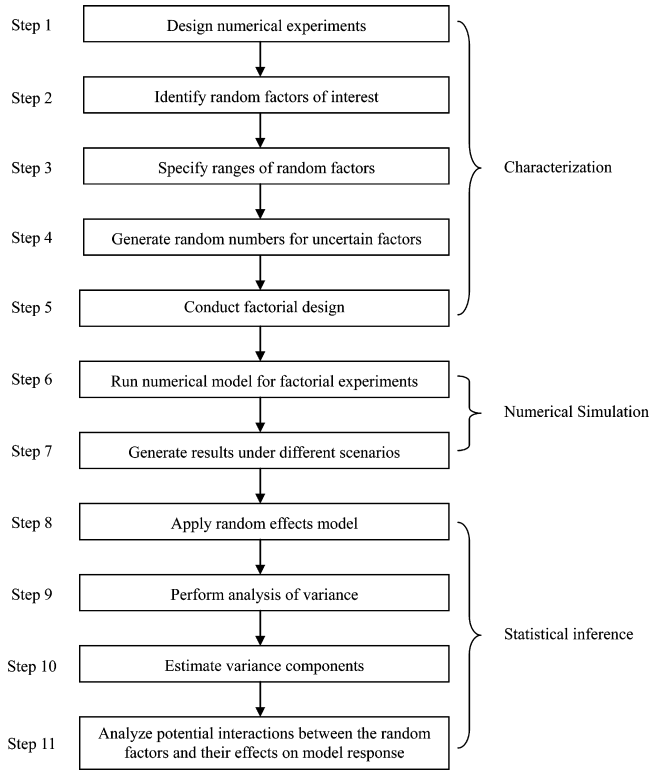

Figure 1. Outline of the proposed methodology.

3. CASE STUDY

3.1. Overview of the Study System. To illustrate the proposed model, a numerical experiment from Lenhard et al.[28] was used in this study. The problem was to simulate the gaseous transport behavior of residual TCE volatilized from a container near the upper boundary of an experimental box and the vapors migrated through a sandy porous medium that had a water table maintained near the lower boundary. TCE vapor concentrations were measured by extracting gas samples from a regularly spaced assemblage of measurement ports. Figure 2 presents the simulation domain with an area of 200 cm (x direction) × 100 cm (y direction) × 7.5 cm (z direction). The domain was discretized into 20 × 20 = 400 grids, resulting in 21 × 21 = 441 nodes. The low permeability and porosity zones were placed on either side of the contaminant vapor source to mimic the presence of a container with impermeable sides and permeable top and bottom, which were used to direct TCE vapors into the sand. Groundwater flowed from right to left due to an imposed

dx.doi.org/10.1021/ie4012003 | Ind. Eng. Chem. Res. 2013, 52, 8602−8611

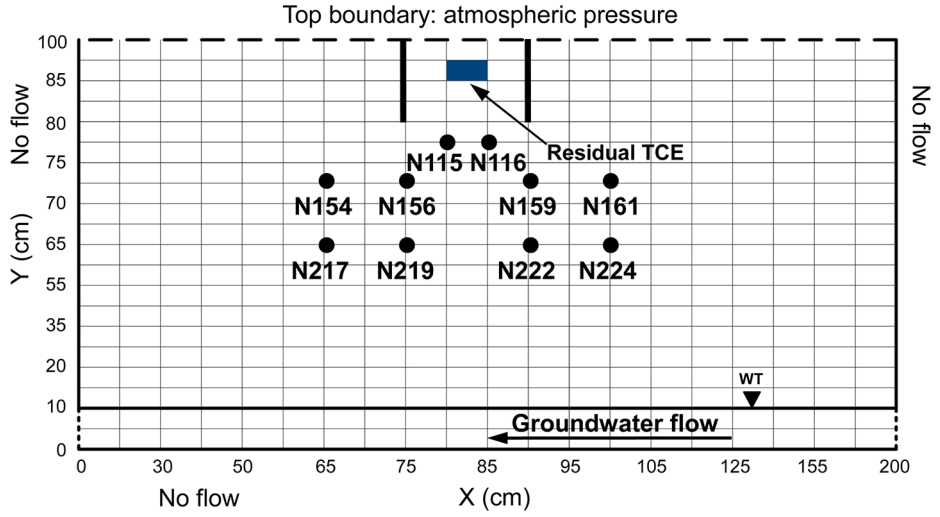

Figure 2. Simulation domain.

head differential. The spatial and temporal distribution of TCE concentrations in the gas phase were measured using 10 checkpoints placed below the source zone.

The input parameters used in numerical simulation are provided in Table 1. Four parameters, including intrinsic permeability ranging from 2.30×10^{-8} to 2.10×10^{-6} cm^2, porosity ranging from 0.26 to 0.47, molecular diffusion in gas ranging from 0.009 to 0.081 cm^2 s^{-1}, and dimensionless Henry's law constant ranging from 0.236 to 0.422 were considered as random factors of interest for the TCE vapor transport in the porous media. Their main and interaction effects on gaseous TCE concentrations could be analyzed through the proposed model.

Table 1. Input Parameters Used in Numerical Simulation

parameter	value	unit
water density, ρ^W	0.9982	g cm^{-3}
NAPL density, ρ^N	0.00553	g cm^{-3}
gas density, ρ^G	0.00117	g cm^{-3}
Water viscosity, μ^W	0.01	P
NAPL viscosity, μ^N	0.0002	P
gas viscosity, μ^G	0.0002	P
residual water saturation, S_{Wr}	0	
residual gas saturation, S_{Gr}	0	
residual NAPL saturation, S_{Nr}	0.20	
gas/water interfacial tension, σ_{GW}	72.75	dyn cm^{-1}
NAPL/water interfacial tension, σ_{NW}	31.74	dyn cm^{-1}
gas/NAPL interfacial tension, σ_{GN}	47.50	dyn cm^{-1}
pressure scale for drainage, a_d	0.156	1 cm^{-1}
pressure scale for imbibition, a_d	0.156	1 cm^{-1}
pore connectivity parameter, η	4.26	
molecular diffusion in water, D_m^W	0.00001	cm^2 s^{-1}
equilibrium concentration of the NAPL component in the water phase (solubility limit), $\bar{\rho}_m^W$	0.0011	g cm^{-3}
equilibrium concentration of the NAPL component in the gas phase (solubility limit), $\bar{\rho}_n^G$	0.00052	g cm^{-3}

3.2. Results and Discussion. A numerical model was first used in this study to simulate the gaseous TCE transport experiment. Figure 3 presents the evolution of the TCE gas plume in the sandy porous medium for t = 12, 15, and 18 h. At t = 12 h, the TCE vapors had a slight vertical movement, indicating that vapor advection played an important role in the gaseous TCE transport processes at the early times. The TCE concentrations in the gas phase near the contaminant source were highest, which was a result of diffusion directly from the TCE residual. At t = 15 h, the TCE gas plume moved downward due to the high vapor pressure and molecular mass of TCE but had not yet reached the water table located near the bottom boundary (as shown in Figure 2). At t = 18 h, the TCE vapors had reached the water table and begun spreading along its surface. The gaseous TCE concentrations became lower compared with those at t = 12 and 15 h, indicating the effects of gas diffusion.

To investigate the effects of random factors including permeability, porosity, molecular diffusion in gas, and Henry's law constant on the transport of the TCE vapor plume originating from a residual TCE source in porous media, 162 simulation runs were performed for t = 12, 15, and 18 h, respectively. The results indicate that variations of these random factors can cause a significant difference in the gaseous TCE concentrations (see Figures S1−S10 in the Supporting Information). It is thus necessary to investigate their effects and identify the dominant factors as well as their latent interactions. Since the levels of the four factors under consideration were chosen randomly, the four-factor random effects model was used for the analysis of variance.

Examination of residuals plays an important role in any analysis of variance. Plotting the residuals in time order of data collection is helpful in detecting correlation between the residuals as well as the outliers that can seriously distort the analysis of variance. The plots of residuals versus simulation runs for all checkpoints are shown in Figures S1−S10 in the Supporting Information. These plots reveal that the residuals contain no obvious patterns, implying that there is no violation of the independence assumption on the errors. Furthermore, the majority of residuals fall within ±1, and all of them fall within ±2. Since a residual larger than 3 or 4 standard deviations from zero is considered as a potential outlier, the plots give no indication of outliers, which should cause no concern. Thus, the analysis of variance is legitimate and reliable.

The analysis of variance of the random effects model for the checkpoint N115 at t = 12, 15, and 18 h is reported in Table 2. Factors A, B, C, and D represent the four factors: permeability, porosity, molecular diffusion in gas, and dimensionless Henry's law constant, respectively. Their interactions are denoted as AB, AC, and BC. The results indicate that the interaction terms

dx.doi.org/10.1021/ie4012003 | Ind. Eng. Chem. Res. 2013, 52, 8602−8611

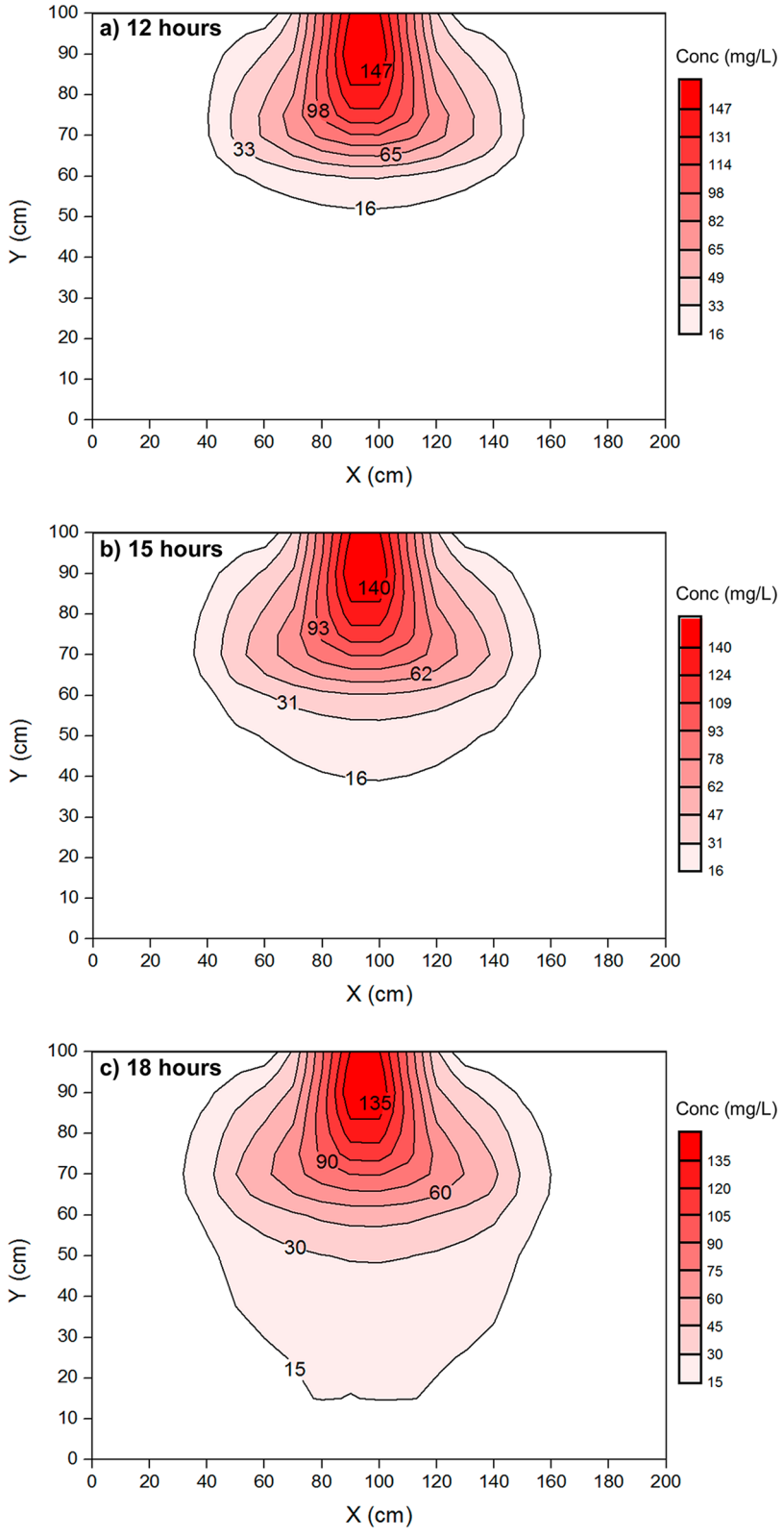

Figure 3. Distributions of gaseous TCE concentrations at t = 12, 15, and 18 h.

related to factor D are negligible in the random effects model, since they all have little effect on the TCE vapor concentrations. According to the analysis of variance, the TCE vapor concentrations are not sensitive to variations in factor D but are sensitive to factors A, B, and C as well as their interactions. Particularly, factor C has the smallest P-values and the largest estimates of variance components for t = 12, 15, and 18 h, implying that it has the most significant influence on the TCE vapor concentrations. The effect of factor B is significant for t = 12 and 15 h but not for t = 18 h. The variance components were estimated through the analysis of variance method. The results show that a negative estimate of a variance component is

dx.doi.org/10.1021/ie4012003 | Ind. Eng. Chem. Res. 2013, 52, 8602−8611

Table 2. Analysis of Variance of the Random Effects Model for Checkpoint N115

source	t = 12 h mean square	P value	variance component	t = 15 h mean square	P value	variance component	t = 18 h mean square	P value	variance component	expected mean square for each term
A: permeability	689.110	0.029	10.994	354.930	0.027	5.629	211.300	0.025	3.360	(8) + 18 (6) + 18 (5) + 54 (1)
B: porosity	666.920	0.025	10.715	726.590	0.031	11.675	325.440	0.248	2.947	(8) + 18 (7) + 18 (5) + 54 (2)
C: molecular diffusion in gas	6483.200	0.000	117.268	4969.040	0.000	89.717	4612.290	0.002	82.046	(8) + 18 (7) + 18 (6) + 54 (3)
D: Henry's law constant	0.030	0.954	−0.011	0.020	0.966	−0.009	0.010	0.976	−0.007	(8) + 54 (4)
AB	16.810	0.000	0.899	11.640	0.000	0.620	7.370	0.000	0.388	(8) + 18 (5)
AC	79.250	0.000	4.368	39.800	0.000	2.184	22.860	0.000	1.248	(8) + 18 (6)
BC	72.130	0.000	3.972	84.990	0.000	4.695	159.320	0.000	8.830	(8) + 18 (7)
error	0.630		0.633	0.490		0.486	0.390		0.386	(8)

produced for factor D, which is certainly not reasonable because by definition variances are nonnegative. This is considered as one of the drawbacks of the analysis of variance method. Thus, there are a variety of methods to tackle this problem.[30] One alternative is to assume that the negative estimate means that the variance component is zero, which is used as a means in this study. The expected mean square was examined for each term in the random effects model. For example, the expected mean square for factor C at t = 12 h can be obtained as follows: (8) + 18(7) + 18(6) + 54(3) = 0.633 + 18(3.972) + 18(4.368) + 54(117.268) = 6483.225. The analysis of variance of the random effects model for the other checkpoints is provided in Tables S1−S9 in the Supporting Information.

Due to the fact that temporal and spatial variability in the TCE vapor concentrations can result in different effects of factors, Figure 4 presents the variations of factor effects for the checkpoints N115 and N224 at t = 12, 15, and 18 h. In light of the estimates of variance components, the results reveal that the significance of the effects of factor C and its interaction AC is decreasing for the checkpoint N115 but is increasing for the checkpoint N224 at t = 12, 15, and 18 h. For the checkpoint N224, factor A has the most remarkable effect on the TCE vapor concentration for t = 12 h, while the effect of factor C become the most significant one for t = 15 and 18 h. Therefore, the effects of factor vary in a different time and location.

Figure 5 shows the main effect plots for the checkpoints N115 and N224 at t = 12 h. It is indicated that each factor has three randomly chosen levels. The plots reveal that factor C with a relatively steep slope has the largest negative influence on the TCE vapor concentration for the checkpoint N115. The concentration would be reduced from 29.861 to 13.118 mg/L and then from 13.118 to 9.245 mg/L, if factor C varies from its low level of 0.026 to its midlevel of 0.055 cm^2/s and then from its midlevel of 0.055 to its high level of 0.077 cm^2/s, respectively. For the checkpoint N224, there would be a negative effect on the TCE concentration when factor A varies from its low level of 9.280×10^{-8} to its midlevel of 6.868×10^{-7} cm^2; however, the effect of factor A would become positive between its midlevel of 6.868×10^{-7} and its high level of 1.349×10^{-6} cm^2. In comparison, factor D with a slight slope has no influence on the TCE vapor concentrations for either N115 or N224. Figure 6 presents the interaction plots of AB, AC, and BC for the checkpoints N115 and N224 at t = 12 h. The plots expose that, for the checkpoint N115, a variation of factor C from its lower level to its midlevel would result in a remarkable reduction in the TCE vapor concentration when either of factors A or B is at the low level. For the checkpoint N224, the TCE vapor concentration would be sensitive to the variation of factor A from its low level to its midlevel no matter what levels factors B and C are at.

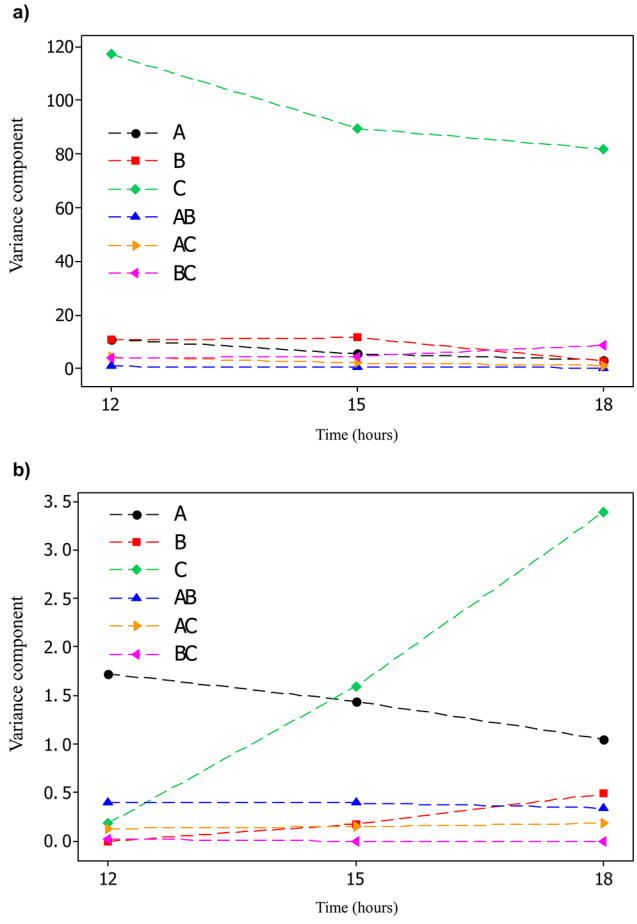

Figure 4. Variations of effects of six factors for checkpoints N115 and N224 at t = 12, 15, and 18 h.

In this study, the random effects model was introduced to investigate the effects of random factors on the TCE vapor concentrations. Accordingly, inferences were made about the entire population of factor levels. When the levels of factors are specified deliberately rather than randomly sampled from an infinite population of possible levels, the conventional fixed effects model can be used to examine the fixed factors, implying that the inference space is the specific set of factor levels investigated. To compare with the random effects model, the fixed effects model was also used to explore the factors with each having two levels. Taking the checkpoint N115 as an example,

dx.doi.org/10.1021/ie4012003 | Ind. Eng. Chem. Res. 2013, 52, 8602−8611

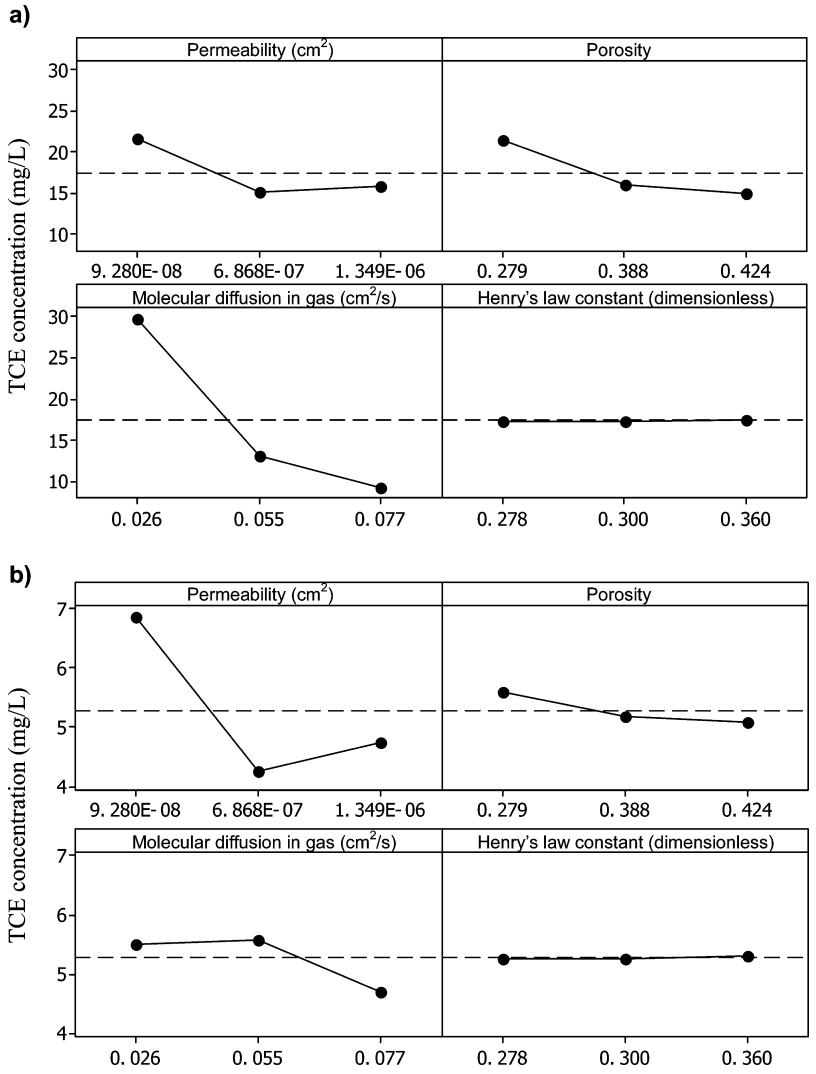

Figure 5. Main effect plots for checkpoints N115 and N224 at t = 12 h.

the analysis of variance of the fixed effects model for the checkpoint N115 was reported in Table S10 in the Supporting Information. It is indicated that factors A, B, and C have the remarkable main effects on the TCE concentrations at t = 12, 15, and 18 h. Different from the random effects model, the effects of factor B are significant all the time rather than only at t = 12 and 15 h. In terms of the joint effects of factors, interactions AB and BC have the prominent influences on the TCE vapor concentrations for t = 12, 15, and 18 h; the effect of interaction AC is only considerable at t = 12 h, which is different from the random effects model.

Figure 7 presents the single and joint effects plots generated from the fixed effects model for the checkpoint N115 at t = 12 h. The plots reveal that factor C has the most significant negative influence on the TCE vapor concentration, which matches that from the random effects model. Additionally, the TCE vapor concentration would be sensitive to the variation of factor C from its low level to its high level when either of factors A and B is at its low level. Consequently, the results indicate that there would be a difference in the conclusions drawn from the fixed and random effects models due to the fact that the statistical inferences are made about the entire population of factor levels in the random effects model while they are made about the specific levels of interest in the fixed effects model. Moreover, the two-level fixed effects model assumes that the response is linear over the range of the factor levels chosen. However, many real-world problems involve the nonlinear relationships between the factors and the model response. The two-level fixed effects model can hardly address the nonlinear effects. In comparison, the random effects model is capable of detecting the curvature in the factor-response relationship. Consequently, the proposed random effects model is effective in revealing the latent interactions between random factors and their nonlinear effects on the model response.

As the number of random factors increases in large-scale problems, the required number of experimental runs rises exponentially, resulting in a high computational effort. Therefore, it is indispensable to apply a factor screening strategy to identify the important factors and discard those unimportant ones in the first place, which is effective in reducing the computational burden. Since the results of the numerical simulation provide the bases for the analysis of variance, the accuracy of the simulation model determines the applicability of the proposed simulation-based random effects model. In real-world problems, the numerical model should be calibrated such that the simulated results would be close to the observed ones (from on-site monitoring program). The reliability of such a simulation model can be enhanced, leading to an improved performance of the random effects model.

dx.doi.org/10.1021/ie4012003 | Ind. Eng. Chem. Res. 2013, 52, 8602−8611

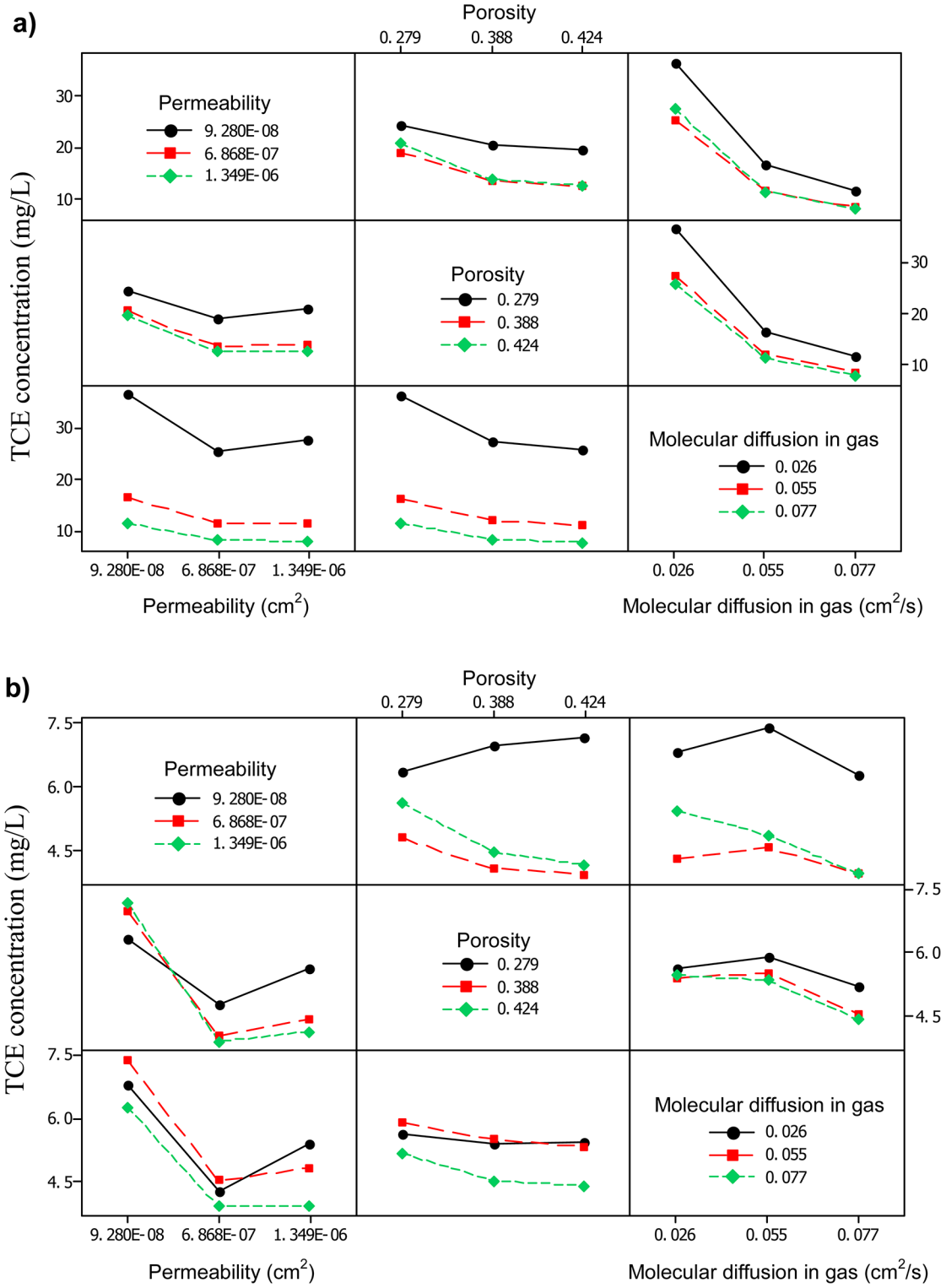

Figure 6. Interaction plots for checkpoints N115 and N224 at t = 12 h.

4. CONCLUSIONS

In this study, a simulation-based random effects model was developed to investigate the interaction effects of random factors on the gaseous transport of VOCs in the unsaturated zone. The proposed methodology integrated characterization, simulation, and statistical analysis within a general framework, which had the advantages of addressing the inherent randomness of modeling parameters in simulating the gaseous transport of VOCs in the subsurface and of analyzing their interaction effects on the VOC vapor concentrations.

A numerical experiment on the transport behavior of TCE vapors in the unsaturated porous media was used to illustrate the proposed model. The results indicated that random factors would have different influences on the gaseous TCE concentrations, and their effects would vary along with temporal and spatial variability in the TCE vapor concentrations. The

dx.doi.org/10.1021/ie4012003 | Ind. Eng. Chem. Res. 2013, 52, 8602−8611

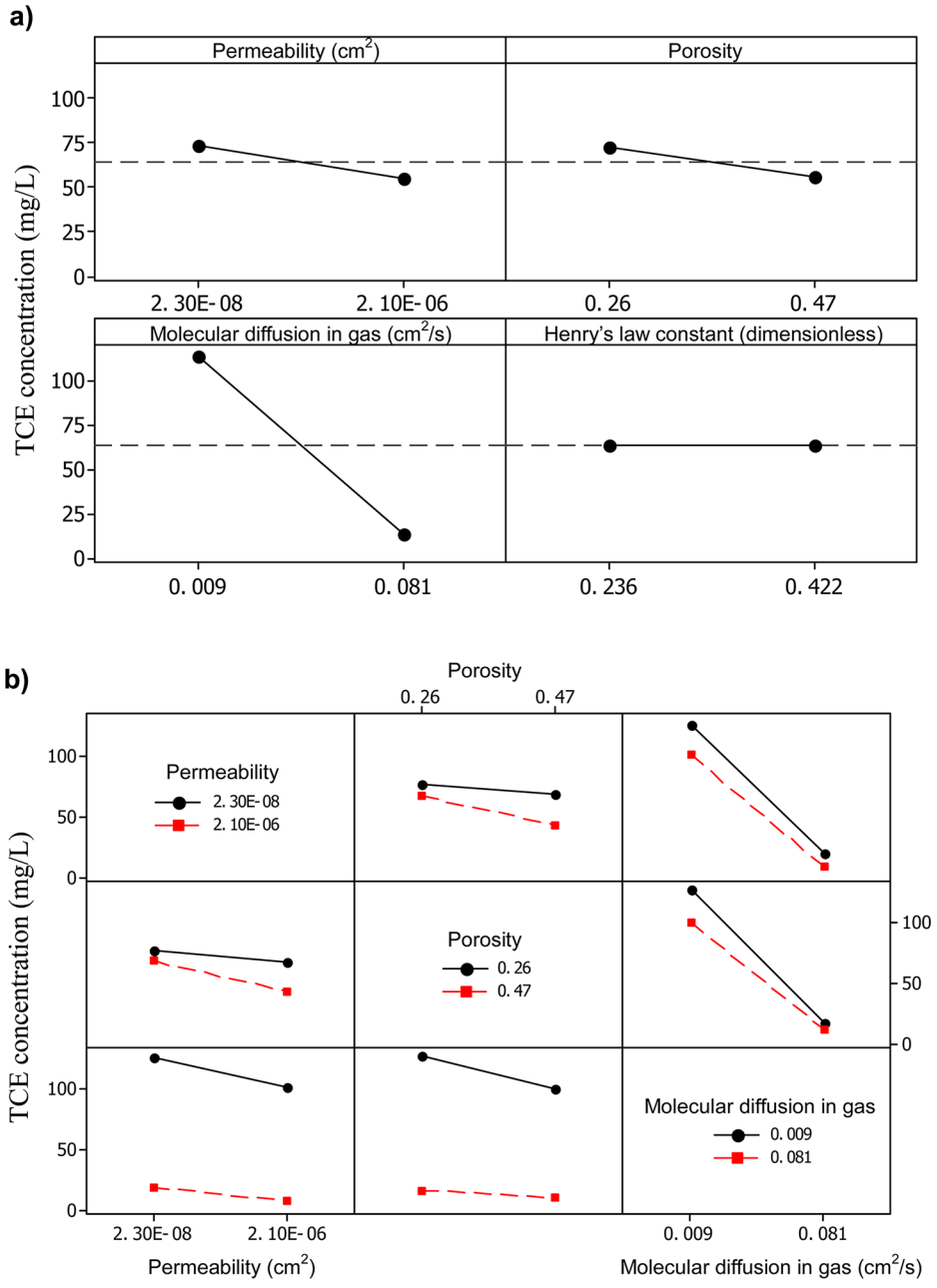

Figure 7. Single and joint effects plots generated from the fixed effects model for checkpoint N115 at t = 12 h.

results obtained from the random effects model were compared to those from the most popular two-level fixed effects model. Such a comparison revealed that conclusions drawn from the two models would be different since the statistical inferences were made in different ways. Moreover, the random effects model was capable of detecting the curvature in the response function, while it was impossible to reflect such a nonlinear effect with the two-level fixed effects model due to its assumption of linearity over the range of factor levels. Therefore, the random effects model was desired when the investigated factors were random and they had nonlinear effects on the model outputs.

■ ASSOCIATED CONTENT

Ⓢ Supporting Information

Simulation results and residuals for 10 checkpoints, analysis of variance of the random effects model for 9 checkpoints, and analysis of variance of the fixed effects model for checkpoint N115. This material is available free of charge via the Internet at http://pubs.acs.org.

■ AUTHOR INFORMATION

Corresponding Author

*Tel.: +1 306 585 4095. Fax: +1 306 585 4855. E-mail: huang@iseis.org.

Notes

The authors declare no competing financial interest.

■ ACKNOWLEDGMENTS

This research was supported by the Major Project Program of the Natural Sciences Foundation (51190095) and the Natural Science and Engineering Research Council of Canada. The authors would like to express thanks to the editor and the

anonymous reviewers for their constructive comments and suggestions.

REFERENCES

(1) Thomson, N. R.; Sykes, J. F.; Vliet, D. V. A numerical investigation into factors affecting gas and aqueous phase plumes in the subsurface. *J. Contam. Hydrol.* **1997**, *28*, 39−70.
(2) Falta, R. W.; Javandel, I.; Pruess, K.; Witherspoon, P. A. Density-driven flow of gas in the unsaturated zone due to the evaporation of volatile organic compounds. *Water Resour. Res.* **1989**, *25*, 2159−2169.
(3) Jang, W.; Aral, M. M. Density-driven transport of volatile organic compounds and its impact on contaminated groundwater plume evolution. *Transport Porous Med.* **2007**, *67*, 353−374.
(4) Molins, S.; Mayer, K. U.; Amos, R. T.; Bekins, B. A. Vadose zone attenuation of organic compounds at a crude oil spill site − Interactions between biogeochemical reactions and multicomponent gas transport. *J. Contam. Hydrol.* **2010**, *112*, 15−29.
(5) Jellali, S.; Benremita, H.; Muntzer, P.; Razakarisoa, O.; Schafer, G. A large-scale experiment on mass transfer of trichloroethylene from the unsaturated zone of a sandy aquifer to its interfaces. *J. Contam. Hydrol.* **2003**, *60*, 31−53.
(6) Mendoza, C. A.; Frind, E. O. Advective-dispersive transport of dense organic vapors in the unsaturated zone. 1. Model development. *Water Resour. Res.* **1990a**, *26*, 379−387.
(7) Mendoza, C. A.; Frind, E. O. Advective-dispersive transport of dense organic vapors in the unsaturated zone. 2. Sensitivity analysis. *Water Resour. Res.* **1990b**, *6*, 388−398.
(8) Ong, S. K.; Culver, T. B.; Lion, L. W.; Shoemaker, C. A. Effects of soil moisture and physical-chemical properties of organic pollutants on vapor-phase transport in the vadose zone. *J. Contam. Hydrol.* **1992**, *11*, 273−290.
(9) Conant, B. H.; Gillham, R. W.; Mendoza, C. A. Vapor transport of trichloroethylene in the unsaturated zone: Field and numerical modeling investigations. *Water Resour. Res.* **1996**, *32*, 9−22.
(10) Fen, C. S.; Abriola, L. M. A comparison of mathematical model formulations for organic vapor transport in porous media. *Adv. Water Resour.* **2004**, *27*, 1005−1016.
(11) Christophersen, M.; Broholm, M. M.; Mosbæk, H.; Karapanagioti, H. K.; Burganos, V. N.; Kjeldsen, P. Transport of hydrocarbons from an emplaced fuel source experiment in the vadose zone at Airbase Værløse, Denmark. *J. Contam. Hydrol.* **2005**, *81*, 1−33.
(12) Bohy, M.; Dridi, L.; Schafer, G.; Razakarisoa, O. Transport of a mixture of chlorinated solvent vapors in the vadose zone of a sandy aquifer: Experimental study and numerical modeling. *Vadose Zone J.* **2006**, *5*, 539−553.
(13) Molins, S.; Mayer, K. U. Coupling between geochemical reactions and multicomponent gas and solute transport in unsaturated media: A reactive transport modeling study. *Water Resour. Res.* **2007**, *43*, W05435.
(14) Rivett, M. O.; Wealthall, G. P.; Dearden, R. A.; McAlary, T. A. Review of unsaturated zone transport and attenuation of volatile organic compound (VOC) plumes leached from shallow source zones. *J. Contam. Hydrol.* **2011**, *123*, 130−156.
(15) Abbas, T. R.; Yu, J. H.; Fen, C. S.; Yeh, H. D.; Yeh, L. M. Modeling volatilization of residual VOCs in unsaturated zones: A moving boundary problem. *J. Hazard Mater.* **2012**, *219−220*, 231−239.
(16) Maqsood, I.; Li, J. B.; Huang, G. H. Inexact multiphase modeling system for the management of subsurface contamination under uncertainty. Pract. Period. Hazard., Toxic, Radioact. *Waste Manag.* **2003**, *7*, 86−94.
(17) Zhao, H.; Tonkyn, R. G.; Barlow, S. E.; Peden, C. H. F.; Koel, B. E. Fractional factorial study of HCN removal over a 0.5% Pt/Al_2O_3 catalyst: Effects of temperature, gas flow rate, and reactant partial pressure. *Ind. Eng. Chem. Res.* **2006**, *45*, 934−939.
(18) Lin, Y. P.; Huang, G. H.; Lu, H. W.; He, L. A simulation-aided factorial analysis approach for characterizing interactive effects of system factors on composting processes. *Sci. Total Environ.* **2008**, *402*, 268−277.
(19) See, C. H.; Dunens, O. M.; MacKenzie, K. J.; Harris, A. T. Process parameter interaction effects during carbon nanotube synthesis in Fluidized beds. *Ind. Eng. Chem. Res.* **2008**, *47*, 7686−7692.
(20) Qin, X. S.; Huang, G. H. Characterizing uncertainties associated with contaminant transport modeling through a coupled fuzzy-stochastic approach. *Water Air Soil Poll.* **2009**, *197*, 331−348.
(21) Mabilia, R.; Scipioni, C.; Vegliò, F.; Tomasi Scianò, M. C. Fractional factorial experiments using a test atmosphere to assess the accuracy and precision of a new passive sampler for the determination of formaldehyde in the atmosphere. *Atmos. Environ.* **2010**, *44*, 3942−3951.
(22) Onsekizoglu, P.; Bahceci, K. S.; Acar, J. The use of factorial design for modeling membrane distillation. *J. Membr. Sci.* **2010**, *349*, 225−230.
(23) Wang, S.; Huang, G. H.; Veawab, A. A sequential factorial analysis approach to characterize the effects of uncertainties for supporting air quality management. *Atmos. Environ.* **2013**, *67*, 304−312.
(24) Wu, H.; Feng, T. C.; Chung, T. W. Studies of VOCs removed from packed-bed absorber by experimental design methodology and analysis of variance. *Chem. Eng. J.* **2010**, *157*, 1−17.
(25) Guarnaccia, J.; Pinder, G.; Fishman, M. *NAPL: Simulator Documentation*; National Risk Management Research Laboratory: Ada, OK 74820, EPA/600/R-97/102, 1997.
(26) Pinder, G. F.; Abriola, L. M. On the simulation of nonaqueous phase organic compounds in the subsurface. *Water Resour. Res.* **1986**, *22*, 109S−119S.
(27) Bear, J. *Hydraulics of Groundwater*; McGraw-Hill: New York, 1979.
(28) Lenhard, R. J.; Oostrom, M.; Simmons, C. S.; White, M. D. Investigation of density-dependent gas advection of trichloroethylene: Experiment and a model validation exercise. *J. Contam. Hydrol.* **1995**, *19*, 47−67.
(29) Qin, X. S.; Huang, G. H.; Chakma, A. Modeling groundwater contamination under uncertainty: A factorial-design-based stochastic approach. *J. Environ. Inform.* **2008**, *11*, 11−20.
(30) Montgomery, D. C. *Design and analysis of experiments*, 5th ed.; John Wiley & Sons: New York, 2001.